



# PRELIMINARY FULL SIZE TEST OF A SIMPLIFIED VERSION OF THE CMS LINK ALIGNMENT SYSTEM AT THE ISR HALL

*P. Arce, E. Calvo, C.F. Figueroa, N. García, F. Matorras, T. Rodrigo, I. Vila, A.L. Virto  
Instituto de Física de Cantabria, Santander. Spain*

*M.G. Fernández, A. Ferrando, M.I. Josa, A. Molinero, J.C. Oller  
CIEMAT, Madrid. Spain*

## 1. Introduction

The complete CMS [1] muon alignment system is organized in three blocks:

- The internal alignment of Barrel and Endcap muon chambers [2]
- The internal alignment of the Tracker detector [3]
- The Link system to relate Muon and Tracker alignment systems [2]

All of them contribute to the final accuracy. An experimental study of the system as a whole is essential. Due to the large scale, complexity and cost of the full system this experimental study has to be limited to a full-minimum arrangement that contains all the relevant elements. The planned full scale laboratory setup is shown in Figure 1. The setup is a simplified version of one half of a CMS r-z plane containing all the relevant elements for the position monitoring: a tracker zone, a one half of one active plane of the Barrel system, two Endcap lines and the connection between them and the Link lines.

The precision of the whole system will be obtained by comparison of the data provided by the system itself with direct survey measurements. For this reason a precise and redundant survey network, not shown in the figure, will be built around the setup. The CMS- $\phi$  direction has been set vertically, allowing the most precise measurements by optical levelling. The laboratory is being prepared at CERN in a hall of the ISR (Interaction Storage Ring) zone.

For this test a measurements area has been prepared in the hall, there, we have installed a survey network [4] used for angular measurements. After the construction of this network the different components of the setup are also mounted (laser source and fiducialized 2D position sensors) as well as the DAQ.

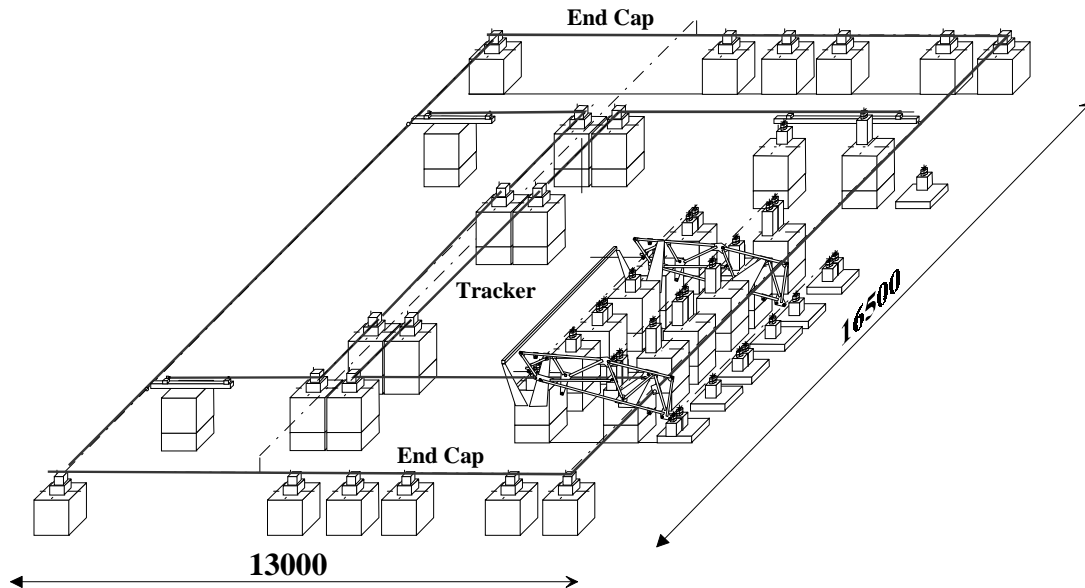


Fig. 1 – Full-scale laboratory test setup of the CMS position monitoring system

The aim of this preliminary test was to evaluate:

- The environmental conditions in the hall
- The stability of the light paths under various conditions
- The resolution in angular measurements making use of the standard CERN survey network

In this document we will give a short reminder of the link system in Section 2. The experimental setup and the DAS will be described in Section 3. A description of measurements and results is given in Section 4. We draw in Section 5 some conclusions.

## 2. Description of the CMS alignment link system

The CMS link alignment system is designed to relate the positions of the CMS inner tracker and the muon systems. The system connects both detectors creating six light paths accessible from both alignment references: tracker alignment wheels and MABs (for the barrel muon detector) or ME1/2 stations (for the end cap muon detector). The light paths define planes in  $\phi$ , every  $60^\circ$ . This segmentation, although redundant, allows a direct reference of each barrel muon sector with the tracker detector and provides direct tracker references to the endcap monitoring system.

Fig. 2 shows a longitudinal cut of the CMS detector with the layout of the link alignment lines. To minimize the interference with other subdetectors the light path follows the inner detector boundaries as shown in the figure and reaches the muon region through radial light channels in the endcap iron disks. The locations of the link points along the path are also indicated in the figure. Four primary points on the MAB structures and four in the ME1/2 stations are used to reference the barrel and endcap alignment systems in this plane. Because of the special location of the ME1/1 stations, extra link points will be used to align these chambers.

At each  $\phi$ , the light beams are generated by two independent laser sources (at  $z \sim \pm 6635$  mm,  $r \sim 627$  mm) attached to the endcap return yoke. Each source produces two laser beams at fixed angle of  $95.7^\circ$  (see Fig. 3). At the inner detector part along the endcap detector boundaries, the optical lines are parallel to  $\eta = 3$  and reach the tracker at  $r \sim 300$  mm. On the tracker alignment wheels, radial periscopes shift the light path from  $\eta = 3$  to match the alignment passages at the outer radius boundaries of the inner tracker detector, allowing optical measurements across this volume.

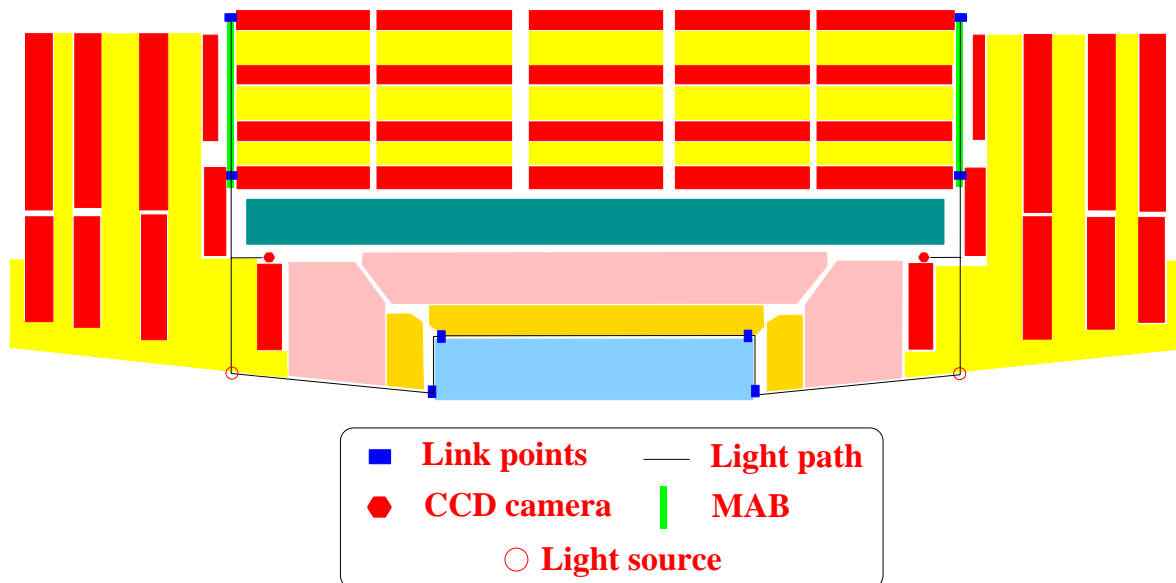


Fig. 2 – Longitudinal cut of the CMS detector with the layout of the alignment lines.

We will concentrate our studies in the link between tracker and MABs, as the link between tracker and ME1/2 stations is equivalent to this one. The measurement of the MAB positions with respect to the tracker alignment wheels uses a total of eight linking points along each light path: four placed at the tracker ends and four at the MAB structures (2 per MAB).

At each z end, the measurement involves:

The position of the laser beam with respect to the tracker wheels ( $x, y$  coordinates). This is obtained at the intersection of the light ray with the 2-D sensor located at the tracker wheels, at  $\eta \sim 3$  (detector 3 in Fig. 3). The origin of the beam from the tracker ( $z$  coordinate) is obtained by distance measurements along  $\eta \sim 3$ . The orientation of the laser beam relative to the tracker is determined by two 2-D measurements at the outer MSGC radial boundary (detectors 4 and 5). The definition of the MAB relative to the radial beam is given by 2-D position sensing detectors, located at the two link points defined on the MAB structure (detectors 1 and 2), that measures the relative position and orientation laser beam-MAB. A radial distance measurement from the origin of the laser beam to the MAB gives the  $r$  coordinate of the link points.

The  $\phi$  orientation MAB-Tracker cannot be directly obtained with this geometry, so it is measured independently by laser levels [5] placed on the MAB and tracker alignment wheels.

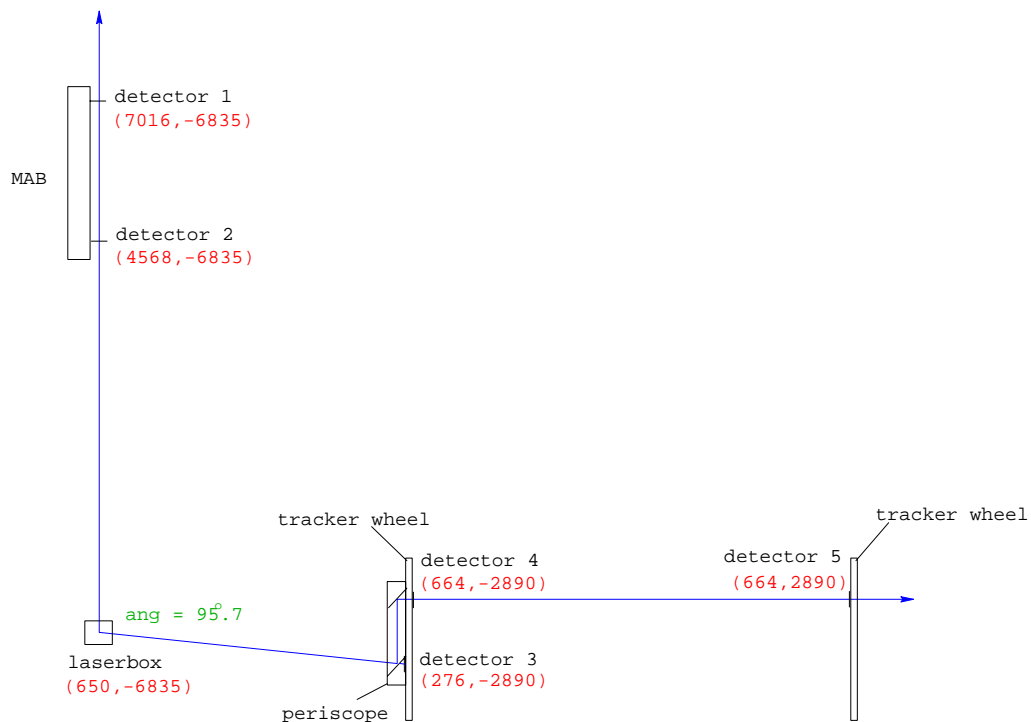


Fig. 3 – Scheme of the light paths linking Central Tracker and MABs.

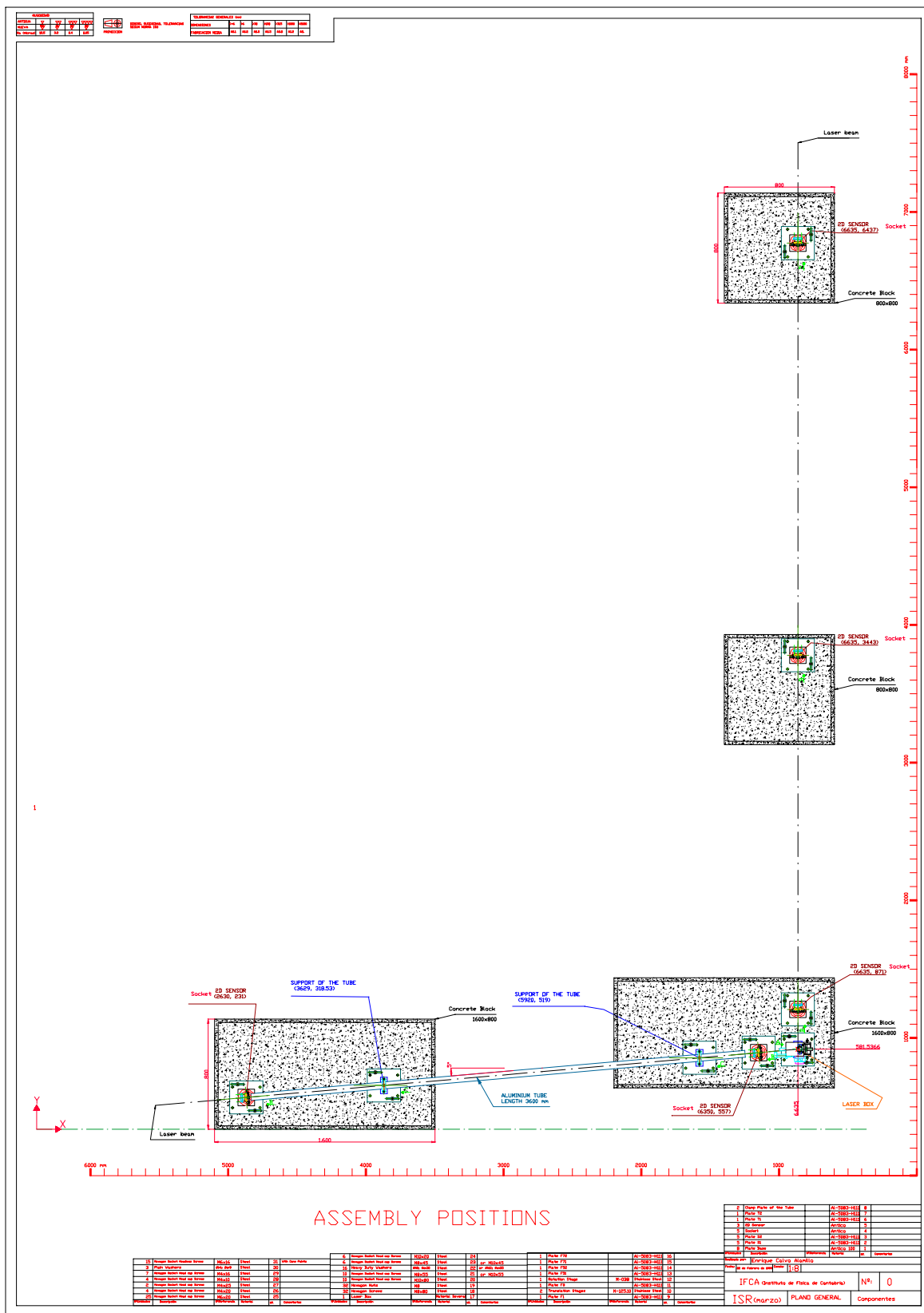


Fig. 4 – Layout of the optical bench.

### 3. Experimental Setup

#### 3.1 The coordinate system

The calibration of the *optical bench* (see Fig. 4), which was equipped with 5 reference sockets, was performed with standard precise survey methods. The distances between the points were measured with an interferometer (20 microns precision). The origin of the co-ordinate system (see Fig. 5) was disposed in such a way that it coincides with the centre of the beamsplitter. The laser source point is located at the intersection of the lines defined by the sockets N5-N3 and N1-N2 (see Fig. 5).

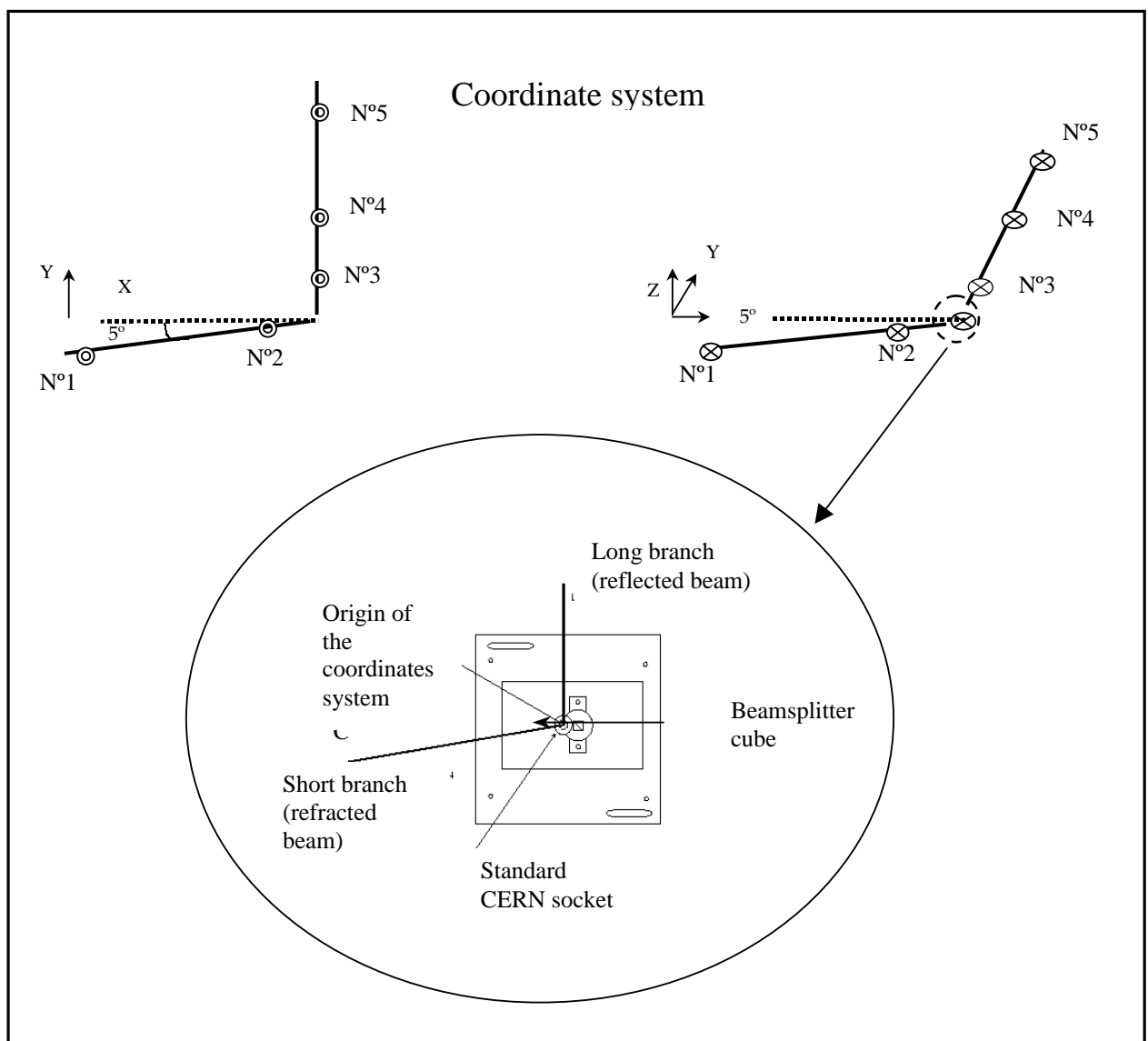


Fig. 5 – Coordinate system. Laser source.

We define the Y axis along the line of the reflected beam, and the X axis along the refracted beam. The Z axis, is perpendicular to the XY plane. In the geometry of the network we tried to reproduce, qualitatively, the geometry of a plane in the real detector. The reference points were the centres of Taylor-Hobson Balls placed on reference sockets, as shown in Fig. 6.

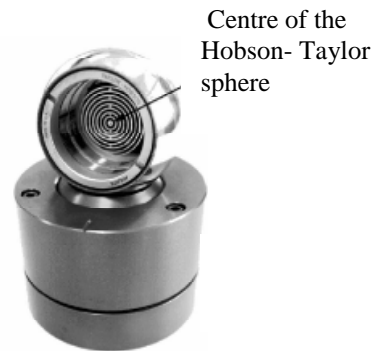


Fig. 6 – Standard socket and Hobson Taylor sphere.

A detailed description of the network calibration is reported in [4]. The three coordinates of the 5 sockets (centres of the Hobson-Taylor spheres) are determined with an error (RMS) of 30  $\mu\text{m}$ .

### **3.1 Components**

#### **3.1.1 Laser source**

The laser source is a unit composed of an optical part (laser diode and beam splitter cube) and a mechanical part (the motorised platforms).

##### **a) Optics**

It consists of two beams generated by a laser diode and a beam splitter. The angle between beams is about 95°. The precise value of this angle is, a priori, unknown. The laser source consists of a pigtailed laser diode coupled to a monomode fibre with final connector type FC/PC. It was controlled by an specific electronics which stabilises the temperature of the laser diode. The wavelength of the laser is 790 nm, and the nominal power is 10 mW. The original beam from the fibre was coupled to a collimator, in order to get a collimated beam all along the working distances. In this way, the quality and the uniformity of the beam is similar in each point of measurement.

##### **b) Platform**

In order to provide the light source with three basics movements, it was mounted on a moving platform. The movements provided by the platform are : 1) vertical displacement along the Z axis; 2) horizontal displacement along the Y axis, and 3) rotation around the Z axis.

### 3.1.2 Position sensors

The 2D position sensors used in the setup were semitransparent amorphous silicon sensors (ALMYs) [6,7,8,9,10]. Prior to the tests, we have characterised the response of the sensors and we have “fiducialized” three of these ALMYs. The fiducialization consists in adjusting the sensor to a very precise mechanical frame [6] that fits perfectly well into the socket, taking the place where the Hobson-Taylor sphere was (see Fig. 7). A precise mechanical method allows then to measure the center of the sensor with respect to the space point previously defined by the center of the Hobson-Taylor sphere with an accuracy of 1  $\mu\text{m}$ . In this way, the centers of the 2D sensors are known, within about 30  $\mu\text{m}$ , with respect to the overall network reference system. Fig. 7 shows the mechanical arrangement of one of the fiducialized sensors placed on its reference socket.

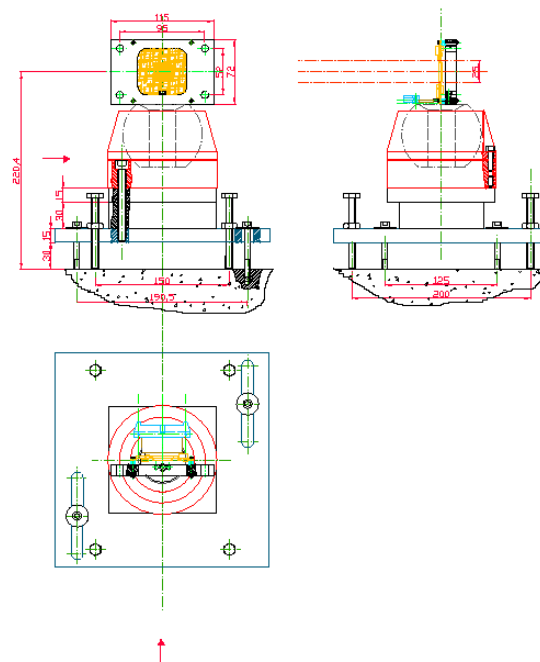


Fig. 7 – Fiducialized ALMY sensor and its reference socket

### 3.1.3 Other components

#### a) Weather station

With this instrument we have measured the environmental variations in the hall: temperature, pressure and relative humidity.



b) Temperature sensors

We had 6 temperature sensors PT-100, with a precision of 0.1 °C, distributed in various places of the set up (sensors, sockets, tube and laser source) in order to control the thermal effect in the mechanics.

c) The light protecting tube

Between points 1 – 2 (see Fig. 4 and 5) we had two auxiliary points in order to hold the tube. This points were not measured. We used the tube as a protector of the laser light in one of the arms, to evaluate any eventual improvement in the beam light stability. The tube was made of PVC, and has a length of 3700 mm.

### 3.3 Data Acquisition System

The signals of the transparent position sensors and the temperature sensors are digitalized by the electronics boxes. These boxes are communicated via the protocol RS-485. A conversion from RS-485 to RS-232 is necessary to establish the communication with the serial port of a PC and has been done through ADAM modules. The movements of the laser source are controlled by a board motor controller (PI-C-842.40) located at the PC. For control of the instruments and of the data acquisition a software module was written in LabView [11]. A layout of the data acquisition and control system used in the test is shown in Fig. 8.

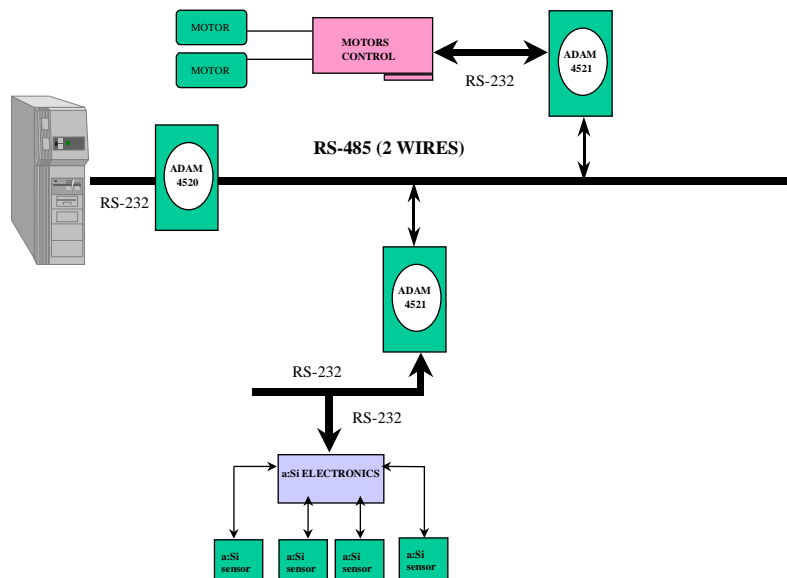


Fig. 8 – Layout of the DAS and control system used in this work.

## 4. Measurements and Results

### 4.1 Environmental conditions in the hall

The hall is located at the ISR tunnel and it is dedicated, in most of its extension, to storage functions. The experimental zone is disposed in a extreme of the hall and it is not isolated from the rest. A system of air conditioning is permanently working. A serie of Na lamps are the only illumination source because in the hall there is not natural light.

With the aim of having a minimum control of the environmental conditions in the hall measurements of temperature, pressure and relative humidity has been done along the five days of the test using a weather station. The result of these measurements are shown in Fig. 9. The pressure and relative humidity variations through the period of five days were 1 % and 13 % respectively. The temperature remained constant and equal to  $(20 \pm 0.5) ^\circ\text{C}$  during the test.

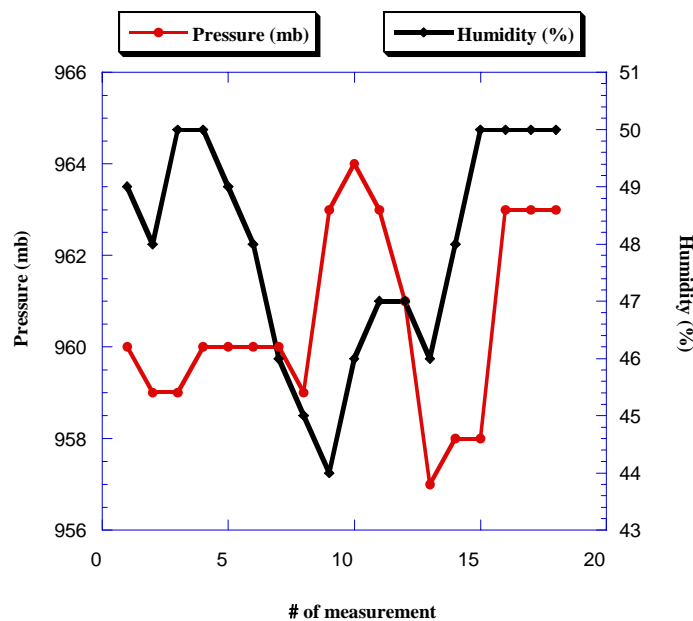


Fig. 9– Environmental conditions of pressure (mb) and humidity (%) during the test (5days).

In order to evaluate the influence in our measurements of different environmental conditions and due to the fact that the measurement zone is not isolated, we induced intentionally several perturbations as: air turbulences, air flows, change in the background illumination, etc... All of them could be probably present in our standard series of measurements. The way to provoke these perturbations was just by opening / closing the outer door, switch on /off the light of the hall.

#### 4.2 Stability measurements

The second goal of the test was to check the stability of the laser beams in both arms of the bench. The influence of the different environmental conditions and perturbations, accidental or intentionally induced by us, has been evaluated. The layout of the experimental setup is shown in Fig. 10.

The laser beams are intercepted by two transparent position sensors. The sensors (A and B) are placed in the farthest survey point of each arm at 4 and 5.9 meters, respectively, from the survey point corresponding to the source. In all the measurements the setup contained two position sensors except one in which we have used a configuration with three sensors, the third installed in the position named B'. In a stability measurement the evolution of the laser spot position detected with the ALMY sensors is periodically recorded. It also allows to determine the precision in the 2D point reconstruction.

Four series of measurements of 12 hours were taken during the night, each of these series were composed of 72 position measurements recorded every 10 minutes (series I, III, IV and VI). Likewise two series of measurements of 3 hours composed by 60 position measurements recorded every 3 minutes (II and V) and a longer serie (VII), of 6 hours of duration composed by 90 position measurements registered every 4 minutes, were taken during the day and under artificial light.

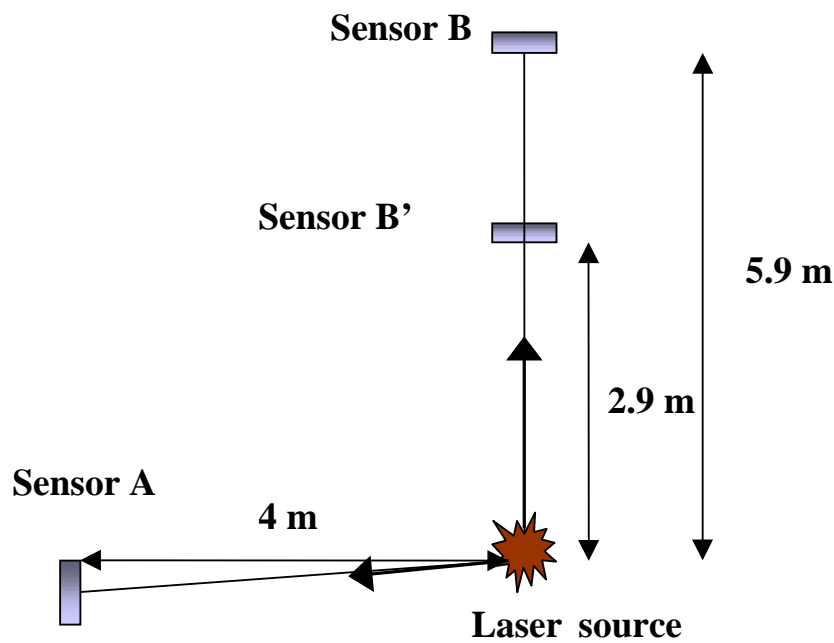


Fig. 10 – Layout of the experimental setup for stability measurements.

The measurements done at night were taken in dark and in the most stable environmental conditions.. In the measurements recorded during the day some perturbations were introduced. In particular, the effects of switching on/off the Na light and inducing possible air flows in the hall were investigated.

We give in Table 1, as an example, a summary of the results for the measurements numbers I (Undisturbed working conditions: night, light off and door closed) and V (introducing disturbances: day, light on, air flows etc.). In the 1<sup>st</sup> column we have indicated the serie. The use/not use of the protector tube in the shorter arm is indicated in the column 2<sup>th</sup> with a Y/ N character. The 3<sup>th</sup> column refers to the position of the ALMY sensors (see Fig. 10) in the network.

In columns 4<sup>th</sup> to 7<sup>th</sup> we present the results of the measurements for the defined sensor: RMS and maximum variation (in microns) of the spot position in the two coordinates X and Y detected by the ALMY sensor during each serie of measurements.

Table 1 –Summary of the stability results

<b>Serie</b>	<b>Tube</b>	<b>Sensor</b>	<b>RMS X (<math>\mu\text{m}</math>)</b>	<b>Max dev X (<math>\mu\text{m}</math>)</b>	<b>RMS Y (<math>\mu\text{m}</math>)</b>	<b>Max dev Y (<math>\mu\text{m}</math>)</b>
<b>I</b>	<b>N</b>	<b>B</b>	<b>4.1</b>	<b>20.1</b>	<b>4.3</b>	<b>29.2</b>
	<b>Y</b>	<b>A</b>	<b>1.6</b>	<b>12.3</b>	<b>1.6</b>	<b>9.8</b>
<b>V</b>	<b>N</b>	<b>B</b>	<b>4.5</b>	<b>28.8</b>	<b>7.6</b>	<b>36.5</b>
	<b>Y</b>	<b>A</b>	<b>10</b>	<b>49</b>	<b>5.0</b>	<b>26.9</b>

The measurements done in undisturbed working conditions (see example in Table 1, serie I) show in all cases X and Y positions distributions having RMS smaller than 5  $\mu\text{m}$ . The reconstructed X and Y positions of the light spot on sensor A as a function of time (measurement number) are shown in Figs. 11a) and b), respectively.

In this example, and after the firts few data points (for wich the system is not yet stabilised), the X position of the spot oscillates around a stable position (9320  $\mu\text{m}$ ), while the Y position shows a small, but systematic, drift-down of mechanical origin. We have not detected such a drift in any other case.

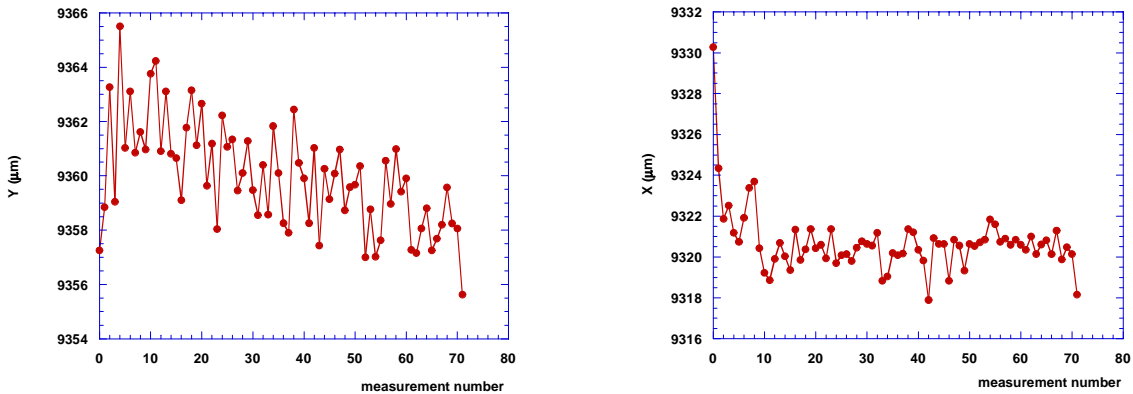


Fig. 11 – a) X position of the spot in the sensor A, Serie I, Fig. 11 – b) Y position of the spot in the sensor A, Serie I

From measurements done introducing disturbances, Table 1 displays the results for measurements number V, as a typical example. The RMS of the X and Y distributions are higher than the ones obtained for undisturbed working measurements. Fig. 12, where the X position of the spot on sensor A is given as a function of the measurement number (time), illustrates what has happened in this particular case: the door of the hall was opened intentionally to induce air turbulences at measurement number 55 (indicated with an arrow in the figure), as a consequence the refraction index of the air changes along the light path and the beam suffers a small deflection. The average in these kind of perturbations have been quantified resulting in an increase in the RMS of the position reconstruction of  $\sim 5 \mu\text{m}$ .

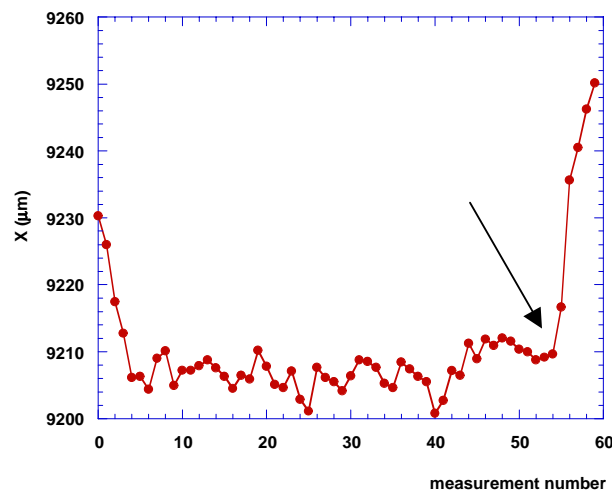


Fig.12 – X positions of the spot in the sensor A, Serie V.

The effect induced by switching on and off the light is illustrated in Fig. 13 where the signal of the spot (in ADC counts) collected at the vertical strips (ADCx) and the horizontal strips (ADCy) of the sensor is plotted as a function of the measured number. The data was taken during 30 minutes at a rate of 1 measurement / minute. The light is off in the measurements 1 to 6. It is turned on for the set 7 to 18. Then off again for measurements 19 to 24 and on from 25 to 29. For point number 30 the light was switched off again.

The fact of switching on/off the light only affects the collected signal at the sensor electrodes but not the resolution in the point reconstruction. In the example in Fig. 13, the RMS (precision) of the reconstructed X position was  $2.8 \mu\text{m}$ .

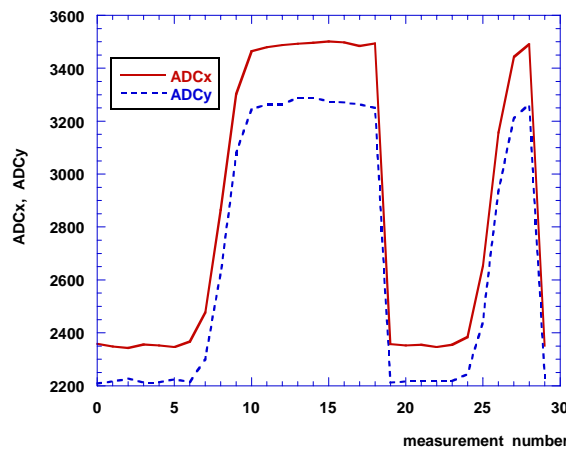


Fig.13 – X and Y ADC counts.

Concerning the light protecting tube the results about its use are not conclusive. We have not found any difference in the measured spatial precisions using or not the protecting tube. The reason could be that the length was not enough: both exits of the tube were about 10-15 cm appart from the light source and the sensor and hence, the protection is far to be perfect.

### 4.3 Angular measurements

To perform absolute angular measurements one needs to use a common reference system for all the optical elements involved. That is provided by the geodesic network. The angle we pretend to measure is the one between both beam lights,  $\alpha$  in Fig. 14. By construction should be around 95 arc. deg. To measure that angle, we used 4 of the 5 points in the network (sensors S1, S2, S3 and S4 in Fig. 14).

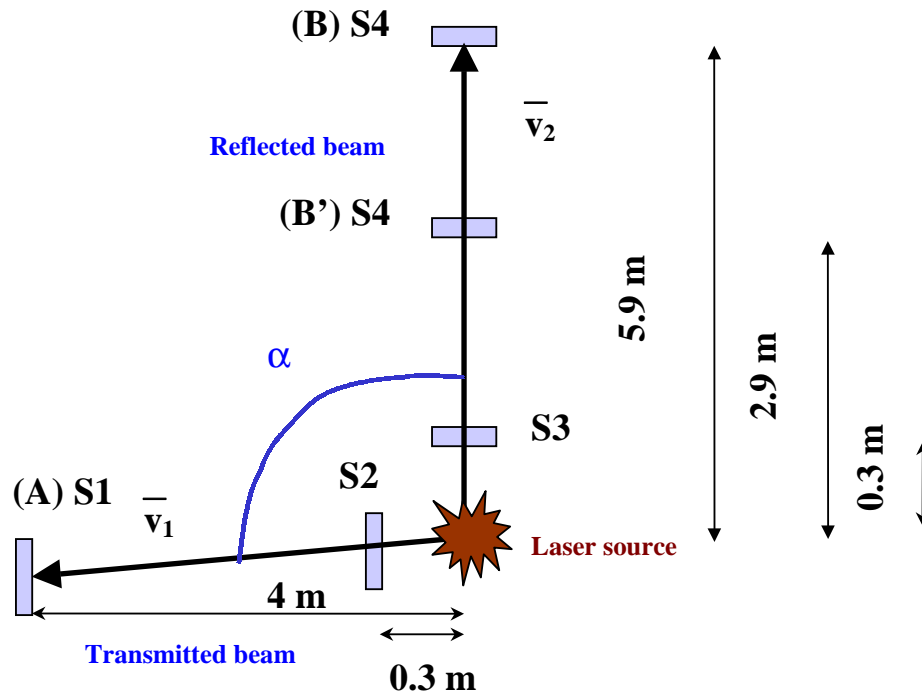


Fig14 – Measurement of the angle between laser beams.

To avoid problems with the deflections induced by the sensors, we never measure in one sensor if it had other in front of it. With the four reconstructed points and using the position detected by the sensors and the corresponding coordinates in the network we obtained two vectors, one for each arm, and then, the angle formed by the two beams is calculated with a scalar product,

$$\alpha = \arccos \frac{\mathbf{v1} \cdot \mathbf{v2}}{|\mathbf{v2}| \cdot |\mathbf{v1}|}$$

We have repeated the measurements of the angle between beams several times, and under different conditions in the hall, to evaluate the precision of the system.

In the first serie of measurements we are work with Na lamps, the second serie was done in dark conditions (the two situations refer as day / night in the Table 2). The results were identical: in both cases the measured precision was 4  $\mu$ rad.

From the analytical expresion of the laser beams angle, we have calculated, by error propagation, the accuracy in the angle reconstruction. The result is 14  $\mu$ rad (Table 2). The most important contribution to this systematic error comes from the network errors. These network errors are of course constant (at least during the few days that the tests lasted) but in the error propagation they become larger or smaller depending on the length of the measurement arms.

For instance, if sensor S4 is used in position B', the resulting accuracy would be 17  $\mu\text{rad}$  instead of 14  $\mu\text{rad}$ .

Table 2 – Measurement of the angle between beams. Summary of the results

	$\langle\alpha\rangle$ arc. deg	Accuracy in the angle reconstruction	RMS( $\alpha$ ) (precision)
<b>Day</b>	95.0196	0.0008 arc.deg. (14 $\mu\text{rad}$ )	0.0002 arc.deg. (4 $\mu\text{rad}$ )
<b>Night</b>	95.0194		0.0002 arc.deg (4 $\mu\text{rad}$ )

## 5 Conclusions

A preliminary full size test of a simplified version containing some relevant elements of the CMS Link Alignment System has been installed in a experimental area of the ISR tunnel at CERN. Previously a calibration bench was prepared with standard precise survey methods.

The environmental conditions, temperature, atmospheric pressure and relative humidity in the hall were controlled revealing quite stable conditions all along the tests period.

The stability measurements done under these conditions show that the light spot on sensors located at about 6 m from the light source are smaller than 5  $\mu\text{m}$ , which satisfies the requirements.

Induced changes in the environmental conditions have different effects. Air flows degrades significantly the spatial resolution ( $\sim 5\mu\text{m}$ ) but the background due to the environmental light does not degrades the resolution in position reconstruction.

A geodesic network defines a reference system common to all optomechanical components and can be used to do absolute measurements of the angle between the two light beams coming out from the splitter. The accuracy in the reconstruction of angles with the help of the geodesic network depends on the errors in the network definition. These errors propagate with a smaller or larger strength depending on the distances between the network points. In our tests, the accuracy in the angle reconstruction is 14  $\mu\text{rad}$  when using 4 m and 5.9 m long arms and 17  $\mu\text{rad}$  for 4 m and 2.9 m arms. We found a precision 4  $\mu\text{rad}$  in the angular reconstruction.

## Acknowledgements

We would like to warmly thank the CERN Positioning Metrology and Surveying group (EST Division) for the the work carry out in the definition of the network as well as the continuous help provided during this test.





## ***References***

- [1] The CMS Collaboration, “The Compact Muon Solenoid Technical Proposal”, CERN/LHCC 94-38, LHCC/P1, December 1994
- [2] The CMS Collaboration, “The Muon Project Technical Design Report”, CERN/LHCC 97-32, CMS TDR 3, December 1997
- [3] The CMS Collaboration, “The Tracker System Project Technical Design Report”, CERN/LHCC 98-6, CMS TDR 5, April 1998
- [4] A. Fronton, J.C. Gayde, K. Nummiaro, “CMS-ISR calibration Bench for the Link System Santander Test Co-ordinates of the reference points” <http://www.cern.ch/SurveExpDiffusion/cms.html>, March 26<sup>th</sup> 1999
- [5] J. Berdugo et al, Nucl. Instr. And Meth. A431 (1999) 437.
- [6] J. Baechler et fils (Geneva), Geodesie Industrielle.
- [7] W. Blumet et al., Nucl. Instr. And Meth. A367 (1995) 413; Nucl. Instr. And Meth. A377 (1996) 404; Max-Planck Institute for Physics MPI-PhE/95-13.
- [8] J. Berdugo et al., Nucl. Instr. And Meth. A 425 (1999) 471
- [9] M.G. Fernández et al., “An in-depth study on semitransparent amorphous silicon sensors”. CIEMAT note 99/890, Nucl. Instr. And Meth. A (in press)
- [10] P. Arce et al., “Gamma irradiation of semitransparent amorphous silicon sensors”. Nucl. Instr. and Meth. A (in press)
- [11] Labview, National Instruments Corporation, Austin, TX 78730-5039.